Journal of Catalysis **207,** 10–22 (2002)
doi:10.1006/jcat.2001.3495, available online at http://www.idealibrary.com on IDEAL®

Characterization of Cobalt Molybdenum Nitrides for Thiophene HDS by XRD, TEM, and XPS

Kenichiro Hada, Junko Tanabe, Shinzo Omi, and Masatoshi Nagai[1]

Graduate School of Bio-Applications and Systems Engineering, Tokyo University of Agriculture and Technology, 2-24 Nakamachi, Koganei, Tokyo 184-8588, Japan

Received June 5, 2001; revised August 29, 2001; accepted December 12, 2001

The activities of the CoMo nitride catalysts, with and without sulfidation, were studied based on the rates of thiophene HDS per catalyst weight and turnover frequency (thiophene converted per irreversibly adsorbed CO). The surface properties, such as morphology, composition, and Co and Mo oxidation state numbers of the catalysts without exposure to air after nitriding were characterized by XRD, TEM, and temperature-programmed reduction. The CoMo nitride catalysts were used after nitriding during the temperature-programmed reaction of mixtures of MoO_3 or $(NH_4)_6Mo_7O_{24}\cdot 4H_2O$ with CoO or $Co(NO_3)_2\cdot H_2O$ with $Co/(Co+Mo) = 0$, 0.25, and 0.5 in a stream of ammonia. Co_3Mo_3N was not produced by nitridation of a mixture of CoO and MoO_3 but was produced from $CoMoO_4$. The TEM analysis showed that Co_3Mo_3N particles (20 to 30 nm) were surrounded by γ-Mo_2N particles (ca. 4 nm) in the catalyst nitrided at 1023 K. An XPS study without argon etching showed that the catalysts nitrided at 773 and 873 K contained Mo^{2+} and Co^{2+}, while the catalysts nitrided at 973–1073 K mainly consisted of Mo^0 and Co^{2+}. The higher activity of the catalyst nitrided at 973 K compared to the other nitrided catalyst is probably due to the formation of a small amount of Co_3Mo_3N before the reaction and the obvious formation after the reaction. The sulfidation of the oxidic catalysts and the catalyst nitrided at 973 K produces stronger active sites of CoMo sulfide rather than Co_3Mo_3N for HDS.

INTRODUCTION

Transition bimetallic nitrides (1–15) have been recently studied as alternatives for Co–Mo and Ni–Mo sulfide catalysts in the hydrodesulfurization (HDS) of kerosene and gas oil. Cobalt molybdenum nitrides were prepared by the temperature-programmed nitriding of a $CoMoO_4$ precursor at a temperature of 973 K (2–9) and of $NH_5(CoOHMoO_4)_2$ via cobalt metal and γ-Mo_2N intermediates at 880 K (12). Furthermore, Fe_3Mo_3N (1, 2) and Ni_2Mo_3N (12, 16) were reported to be prepared by the nitriding of $FeMoO_4$ and $NiMoO_4$ in a stream of N_2 and H_2 with NH_3, respectively. Oyama and coworkers (5, 6) reported the formation of fcc cobalt molybdenum oxynitride from a mixture of $CoC_2H_6O_4$ and MoO_3 even at 892 K as well as the formation of vanadium molybdenum nitrides. Although cobalt molybdenum nitrides and oxynitrides were prepared using a mixture of various oxides, the relationship between the preparation of the cobalt molybdenum nitrides and the parent oxidic precursors was not fully understood. Furthermore, little or no attention has been paid to the surface properties and composition of the cobalt molybdenum nitrides by the temperature-programmed reaction using hydrogen (TPR), X-ray photoelectron spectroscopy (XPS), and XRD. TPR offers detailed information about the surface species of the molybdenum nitrides from the desorption of gases (5, 17–21). In previous studies (17–20) γ-Mo_2N was transformed into β-$Mo_2N_{0.78}$ and Mo metal at about 1100 and 1200 K while desorbing nitrogen and ammonia gases from the unsupported samples during the TPR. Weakly adsorbed NH_X species were also released as ammonia from the molybdenum nitrides, and strongly adsorbed NH_X species were also released as nitrogen gas during the TPR (21). Furthermore, the XPS analysis (4, 18, 22–24) gives information about the distribution and composition of molybdenum in the molybdenum nitrides. Choi *et al*. (22) and Park *et al*. (7) studied the Mo oxidation state on unsupported Mo_2N and 12% Mo/Al_2O_3 nitrided at 973 K and subsequently passivated at room temperature in 1% O_2 in He. They reported that $Mo^{\delta+}(0 < \delta < 4)$ species were selectively produced in the catalysts upon nitridation. Previous papers (18, 20) reported that Mo^{3+} was distributed on γ-Mo_2N particles and Mo^{2+} was found to be highly dispersed as γ-Mo_2N on the alumina of the Mo/Al_2O_3 catalysts nitrided at 973 K in an XPS and TPR study of the relationship between the surface molybdenum and adsorbed nitrogen species in nitrided Mo/Al_2O_3 catalysts (1.0–18.7 wt%). Moreover, the surface composition of the molybdenum nitrides was extensively analyzed by XPS, but not for the cobalt molybdenum nitrides. Thus, the TPR and XPS analyses can shed light on the surface properties of the cobalt molybdenum nitrides. Although CoMo nitrides passivated with 1% O_2 in He were extensively studied as HDS catalysts (3, 5–7, 9–11), they will not have the same surface properties and reactivities as

[1] To whom correspondence should be addressed. E-mail: mnagai@cc.tuat.ac.jp.

0021-9517/02 $35.00

fresh nitrided catalysts because of the formation of oxynitrides on the surface.

In this study, unsupported cobalt molybdenum nitrides were prepared *in situ* and then the HDS activity was measured in order to elucidate the relationships among composition, bulk structure, surface properties, and the HDS activities of the *fresh* nitride catalysts without exposure to air. This study focuses on (i) the relationship between the cobalt molybdenum nitrides and the parent oxidic precursors of the bulk samples during the preparation procedure as determined by XRD, (ii) the morphology and composition of the cobalt molybdenum nitrides as detected by TEM, (iii) the surface composition and the oxidation state numbers of cobalt and molybdenum in the cobalt molybdenum nitrides as revealed by TPR and XPS, and (iv) the activity of the cobalt molybdenum nitrides for the HDS of thiophene at atmospheric pressure compared to cobalt molybdenum sulfide.

EXPERIMENTAL

Preparation of Cobalt Molybdenum Nitrides

The oxidic precursors of the cobalt molybdenum nitrides with the Co/(Co + Mo) ratios of 0, 0.25, and 0.5 were prepared using a mixture of an aqueous solution of cobalt nitrate ($Co(NO_3)_2 \cdot H_2O$, Kishida Chemical Co., 99%) and ammonium heptamolybdate ($(NH_4)_6Mo_7O_{24} \cdot 4H_2O$, Kishida Chemical Co., 99%) (sample code, A), a physical mixture of cobalt nitrate and MoO_3 (B), a physical mixture of CoO and ammonium heptamolybdate (C), and a physical mixture of CoO and MoO_3 (D). The solid products were dried overnight at 373 K and calcined at 773 K for 7 h in dry air. A sample (0.2 g) of the precursors was placed on a porous quartz plate in a 10-mm i.d. quartz microreactor. The sample was oxidized in dry air (49.6 μmol s^{-1}) at 723 K for 1 h, then cooled from 723 to 573 K in dry air (sample code, AF, BF, CF, DF). The catalysts were nitrided by a temperature-programmed reaction from 573 K to the final temperature of 773, 823, 923, 1023, or 1073 K at the rate of 0.0167 K s^{-1} with 49.6 μmol s^{-1} of ammonia (99.99%), maintained at the final temperature for 3 h, and then in flowing ammonia cooled to 623 K and room temperature, respectively, for the activity measurement and characterization. For the sulfided catalysts, 25S623; 25AF723 was sulfided at 623 K in a stream of 10% H_2S/H_2 (49.6 μmol s^{-1}) for 3 h. 25AS623; 25A973 was sulfided at 623 K in a stream of 10% H_2S/H_2 for 3 h. The preparation conditions and abbreviations of the cobalt molybdenum nitrides and sulfides are given in Table 1.

TABLE 1

Catalyst Compositions and Nitridation Conditions

Catalyst	Composition	Feed mixture[a]	Treatment temp. (K)	Treatment procedure[b]
25A773	25% Co 75% Mo	A	773	E
25A873	25% Co 75% Mo	A	873	E
25A923	25% Co 75% Mo	A	923	E
25A973	25% Co 75% Mo	A	973	E
25A1023	25% Co 75% Mo	A	1023	E
25A1073	25% Co 75% Mo	A	1073	E
0A973	100% Mo	A	973	E
50A973	50% Co 50% Mo	A	973	E
25B973	25% Co 75% Mo	B	973	E
25C973	25% Co 75% Mo	C	973	E
25D973	25% Co 75% Mo	D	973	E
25S623	25% Co 75% Mo	A	623	S
25AS623	25% Co 75% Mo	A	973/623	AS
25AF723	25% Co 75% Mo	A	723	F
25BF723	25% Co 75% Mo	B	723	F
25CF723	25% Co 75% Mo	C	723	F
25DF723	25% Co 75% Mo	D	723	F

[a] A: $Co(NO_3)_2 \cdot H_2O$ and $(NH_4)_6 \cdot Mo_7O_{24} \cdot 4H_2O$. B: $Co(NO_3)_2 \cdot H_2O$ and MoO_3. C: CoO and $(NH_4)_6 \cdot Mo_7O_{24} \cdot 4H_2O$. D: CoO and MoO_3.

[b] E: Nitrided at 773–1073 K in a stream of 49.6 μmol s^{-1}. F: Heated in air at 723 K. S (25S623): Sulfiding 25AF723 at 623 K in a stream of 10% H_2S/H_2 (49.6 μmol s^{-1}) for 3 h. AS (25AS623): Sulfiding 25A973 at 623 K.

Characterization

The catalysts were examined by XRD before and after nitriding. The diffraction patterns were obtained on a RAD-II (Rigaku Co.) instrument with Cu $K\alpha$ radiation ($\lambda = 1.542$ Å). The peaks were identified based on the JCPDS references: MoO_3 (JCPDS: 5-0508; $2\theta = 12.8$, 25.7, and 27.4°; this study, $2\theta = 12.9$, 25.8, and 27.4°), MoO_2 (32-671, $2\theta = 26.1$, 36.9, and 53.2°; this study, $2\theta = 26.0$, 36.9, and 53.6°), γ-Mo_2N (25-1366, $2\theta = 37.4$, 43.5, and 63.2°; this study, $2\theta = 37.4$, 43.5, and 63.0°), β-$Mo_2N_{0.78}$ (25-1368, $2\theta = 37.0$ and 42.9°; this study, $2\theta = 37.8$ and 42.9°), Mo metal (42-1120, $2\theta = 40.5$ and 69.9°; this study, $2\theta = 40.5$, and 69.9°), CoO (43-1004, $2\theta = 36.5$, 42.4, and 61.6°; this study, $2\theta = 36.7$, 42.3, and 61.4°), Co metal (5-0727, $2\theta = 44.8$, 47.6, and 76.0°; this study, $2\theta = 44.8$, 47.5, and 76.0°), Co metal (15-806, $2\theta = 44.3$, 51.6, and 75.9°), $CoMoO_4$ (21-868 and 25-1434, $2\theta = 14.2$, 26.7, and 28.5°; this study, $2\theta = 14.2$, 26.5, and 28.5°), and Co_9S_8 (19-364, $2\theta = 29.9$ and 52.0°; this study, $2\theta = 29.9$ and 52.2°). Co_3Mo_3N had the peaks at $2\theta = 35.5$, 40.1, 42.6, 46.6, and 72.8°, as reported by Jackson *et al.* (2) and Kim *et al.* (3). The peaks of cobalt molybdenum oxynitride were identified by comparison with the broad peaks at $2\theta = 37.0$, 43.0, and 63.0° reported by Yu *et al.* (5). Co_2N peaks were reported to be observed at $2\theta = 45.8$, 50.6, and 51.9° (25), and Co_4N at $2\theta = 43.6$, 50.6, and 74.6° (26); 43.8, 50.9, and 75.0° (27).

The morphology of the catalysts was determined using a JEM-2000F transmission electron microscope (JEOL Co.) operating at 200 kV and equipped with an energy-dispersive X-ray spectrometer (EDS). The catalysts were crushed using an agate pestle and mortar, dispersed in ethanol with an ultrasonic apparatus, placed on a copper microgrid,

and transferred to the analysis chamber in the TEM. The amount of cobalt and molybdenum atoms was calculated from the Co/Mo ratio of the catalysts by EDS. Although the nitrogen signal could be monitored in the EDS analysis, the atomic ratios of N/Mo and N/Co were not determined because of errors in the nitrogen determination. The BET surface areas of the catalysts were measured using an Omnisorp 100CX (Beckman Coulter Co.) at liquid-nitrogen temperature after the catalysts were evacuated at 473 K and 1.3×10^{-4} Pa for 2 h. The quantity of CO chemisorbed on the surface of the catalysts was determined by conventional volumetric analysis. Before measuring the CO uptake, the catalysts were pretreated in hydrogen at 623 K for 2 h, degassed at 10^{-2} Pa and 673 K for 2 h, and cooled to room temperature in a vacuum.

During the temperature-programmed reduction (TPR) measurements, the catalyst was heated *in situ* from room temperature to 1220 K at the rate of 0.167 K s^{-1} with 11.2 μmol s^{-1} of hydrogen (99.9999%) after nitriding. Hydrogen was purified through an Indicating Oxitrap (G. L. Science) to remove water and oxygen. The desorbed gases were monitored using a quadrupole mass spectrometer (Quadstar 422, Balzers Co.). Ammonia, water, and nitrogen, present in the desorbing gases during TPR, were qualitatively analyzed at $m/z = 15$, 18, and 28, respectively, using calibration curves.

X-ray photoelectron spectroscopy (XPS) was carried out using a Shimadzu ESCA 3200 photoelectron spectrometer with Mg $K\alpha$ radiation (1253.6 eV, 8 kV, 30 mA). After nitriding, the catalyst was cooled to room temperature in flowing ammonia and not exposed to air in the procedure from the catalyst pretreatment to the XPS measurement. After the stopcocks at each end of the microreactor were closed, the microreactor was transferred to a glovebox in which the atmosphere was exchanged five times with argon (99.9999%) and then filled with argon. The catalyst was removed from the microreactor in the glovebox, mounted onto a sample holder with carbon tape, and then placed in a vial while in the glovebox. The vial was then placed in the XPS prechamber attached glovebag in which the atmosphere was filled with argon. Furthermore, the catalyst on the sample holder was taken out of the vial and then set on a sample rod placed in the prechamber. The XPS analysis was typically done at a pressure of 5×10^{-6} Pa and at a scan speed of 0.33 eV s^{-1}. The spectral region of Mo (and N) and Co was scanned 50 and 80 times, respectively, in order to obtain a good signal-to-noise ratio. Each peak was simulated using a Gaussian function. The baseline corrections determined from the peak fitting of the Co $2p_{3/2}$ and Mo 3*d* lines were carried out using the Shirley method. Argon etching was done for 1 min before the XPS measurement. The C 1*s* binding energy (284.6 eV) was taken as the reference to correct the binding energy of the catalysts. The XPS Mo 3*d* doublets were deconvoluted using an intensity ratio of 2/3 and a splitting of 3.2 eV and then compared with the data reported by Hada *et al.* (18) and Quincy *et al.* (28): Mo^0 (Mo $3d_{5/2}$ binding energy: 227.7 eV, fwhm: 1.2 eV), Mo^{2+} (228.4, 1.4), Mo^{3+} (229.3, 1.5), Mo^{4+} (230.1, 1.6), Mo^{5+} (231.6, 1.7), and Mo^{6+} (233.0, 1.7). In the Co 2*p* spectra, only the Co $2p_{3/2}$ region of all the catalysts was fitted, then compared with the cobalt molybdenum sulfide data by Pawelec *et al.* (29), $CuCo/Al_2O_3$ by Figueiredo *et al.* (30), and Co/Al_2O_3 by Zsoldos *et al.* (31). The XPS binding energies of Co $2p_{3/2}$ for the catalysts were deconvoluted to Co^0 (binding energy: 777.6 eV, fwhm: 1.3 eV), Co^{2+} (779.9, 4.2), Co^{3+} (781.6, 4.7), and the Co^{2+} satellite (786.1, 5.0).

HDS of Thiophene

The flow system for the HDS of thiophene consisted of a single-pass, differential microreactor (4). After nitriding and sulfiding, the catalysts (0.2 g) were cooled to 623 K in a stream of ammonia or 10% H_2S/H_2 without exposure to air, then hydrogen was passed over the catalyst before introduction of the reaction feed. The HDS of thiophene on the catalysts was carried out at 623 K and atmospheric pressure. The reaction feed, consisting of 3.8 vol% thiophene in pure hydrogen (37 μmol s^{-1}), was introduced into the reactor at the rate of 37.2 μmol s^{-1}. A quantitative analysis was performed by injecting a sample from the sampling loop (1 ml) into the gas chromatograph to analyze the amount of thiophene (column: 10% Silicon DC-550) at 348 K and the reaction products (column: VZ-8) at 313 K. The calculation of the HDS rate was based on the moles of thiophene converted at 623 K. $TOF_{integral}$ is the turnover frequency of one site of various Co and Mo species on the cobalt molybdenum compounds formed by the nitridation and sulfidation and was expressed as moles of thiophene converted per moles of CO irreversibly adsorbed at room temperature.

RESULTS AND DISCUSSION

Cobalt Molybdenum Nitrides and Oxidic Precursors

The XRD patterns of the 25A773-1073 catalysts, prepared from a mixture of cobalt nitrate and ammonium heptamolybdate with the Co/(Co + Mo) ratio of 0.25, are shown in Fig. 1. MoO_2 was clearly formed in 25A773 (Fig. 1A) with peaks at $2\theta = 26.0$, 36.9, and 53.2°. A weak peak was observed at $2\theta = 26.0°$ for 25A873–973 (Figs. 1B–1D). The peaks at 37.3 and 43.5° and the small peak at 63.0° demonstrated that γ-Mo_2N was formed in the 25A873–1023 (Figs. 1B–1E) catalysts. For 25A873-1023, the peaks at $2\theta = 37.3$, 43.5, and 63.0° are also close to those at $2\theta = 37.4$, 43.5, and 63.2° for γ-Mo_2N and the broad peaks at approximately $2\theta = 37$, 43, and 63° are probably due to cobalt molybdenum oxynitride in accordance with the data reported by Oyama *et al.* (5, 6). In a previous paper (4), Co_3Mo_3N was reported to be formed in the 50A973 (Co/(Co + Mo) ratio of 0.5) but a small

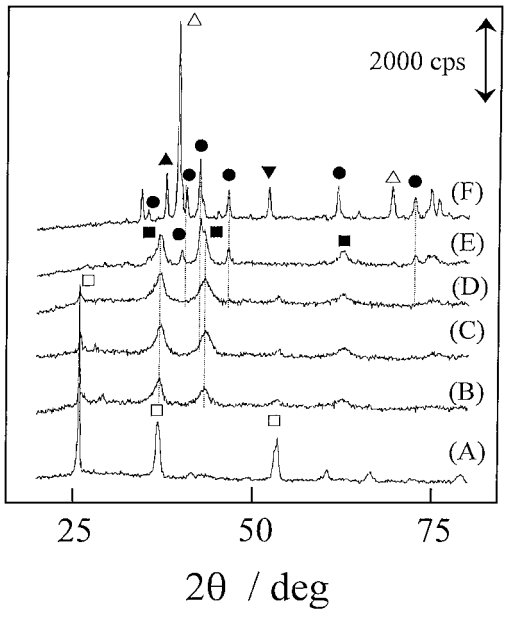

FIG. 1. XRD patterns of cobalt molybdenum oxide and nitrides: (A) 25A773, (B) 25A873, (C) 25A923, (D) 25A973, (E) 25A1023, and (F) 25A1073. Symbols are (●) Co_3Mo_3N, (■) γ-Mo_2N, (▲) β-$Mo_2N_{0.78}$, (□) MoO_2, (△) Mo metal, and (▼) Co metal.

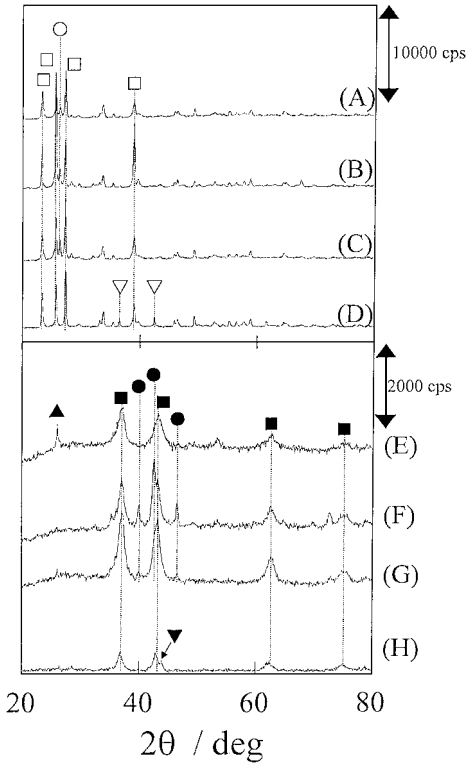

FIG. 2. XRD patterns of cobalt molybdenum oxide and nitrides: (A) 25AF723, (B) 25BF723, (C) 25CF723, (D) 25DF723, (E) 25A973, (F) 25B973, (G) 25C973, and (H) 25D973. Symbols are (●) Co_3Mo_3N, (■) γ-Mo_2N, (▲) MoO_2, (▼) Co metal, (○) $CoMoO_4$, (□) MoO_3, and (▽) CoO.

amount was observed at 43.5° in 25A973. For 25A1023 (Fig. 1E) and 25A1073 (Fig. 1F), the peaks of Co_3Mo_3N were clearly observed at 40.1, 42.6, and 46.6°, in good agreement with those of Co_3Mo_3N previously reported (4) and observed at $2\theta = 40.1$, 42.6, and 46.6° from the ammonolysis of $CoMoO_4$ by Jackson *et al.* (2). Bem *et al.* (1) reported that Fe_3Mo_3N had a cubic structure and Ni_2Mo_3N had an orthorhombic structure. Moreover, Jacobsen (12) reported that the structures of Fe_3Mo_3N and Co_3Mo_3N consisted of corner-shared NMo_6 octahedra with the Fe or Co atoms occupying the sites between the octahedra. For two catalysts, Mo metal was formed as shown by the peaks at $2\theta = 40.5$ and 69.9° with a small amount of β-$Mo_2N_{0.78}$ at $2\theta = 37.8$ and 42.9° and a peak at $2\theta = 52.0°$. The characteristic XRD peak was reported to be ascribed to Co_2N at 51.9° (25) and Co_4N at 50.6° (26) and 50.9° (27) or ascribed to Co metal (cubic) at 51.6° (3). Milad *et al.* (26) described XPS studies in which the Co species were not completely reduced to Co metal during the nitriding of Co_3O_4 at 973 K but to Co_4N. This would explain why various Co and Mo species, such as Co_3Mo_3N, β-$Mo_2N_{0.78}$, Mo metal, and Co nitride, were formed during the nitriding at 1073 K, while Co_3Mo_3N was formed together with γ-Mo_2N (and Co–Mo oxynitride) at 1023 K. The catalyst nitrided at 973 K contained γ-Mo_2N (and Co–Mo oxynitride) with a small amount of Co_3Mo_3N. γ-Mo_2N was formed with MoO_2 during the nitriding at 873 and 923 K.

The XRD patterns of the catalysts prepared according to feed mixture A, B, C, or D, which were oxidized at 723 K in air, are shown in Figs. 2A to 2D. They show the influence of

TABLE 2

Surface Area and Crystalline Size of Cobalt Molybdenum Nitrides

	Monometallic phase		Bimetallic phase	
Sample	Identification	D_C[a] (nm)	Identification	D_C[a] (nm)
25A773	MoO_2	12.1[b]	—	
25A873	γ-Mo_2N	9.4[c]	—	
25A923	γ-Mo_2N	4.5[c]	Co_3Mo_3N	n.d.[f]
25A973	γ-Mo_2N	9.1[c]	Co_3Mo_3N	n.c.[g]
25A1023	β-$Mo_2N_{0.78}$	15.9[d]	Co_3Mo_3N	21.6[h]
25A1073	Mo metal	20.1[e]	Co_3Mo_3N	27.4[h]
50A973	—	n.d.[f]	Co_3Mo_3N	30.3[h]
25B973	γ-Mo_2N	n.d.[f]	Co_3Mo_3N	24.1
25C973	γ-Mo_2N	14.5[c]	Co_3Mo_3N	14.5
25D973	γ-Mo_2N	11.0[c]		
	Co metal	18.3		

[a] By Scherrer equation, $D_c = 0.9\lambda/B\cos\theta$. $\lambda = 1.542$Å, B is the full width at half-maximum corrected for instrumental broadening, and θ is the Bragg angle of the diffraction peak.

[b] MoO_2 (111) phase.

[c] γ-Mo_2N (200) phase and Co-Mo oxynitride.

[d] β-$Mo_2N_{0.78}$ (200) phase.

[e] Mo metal (110) phase.

[f] Not detected.

[g] Not calculated (very weak peak at 43°).

[h] The peak of Co_3Mo_3N phase at 42.6°.

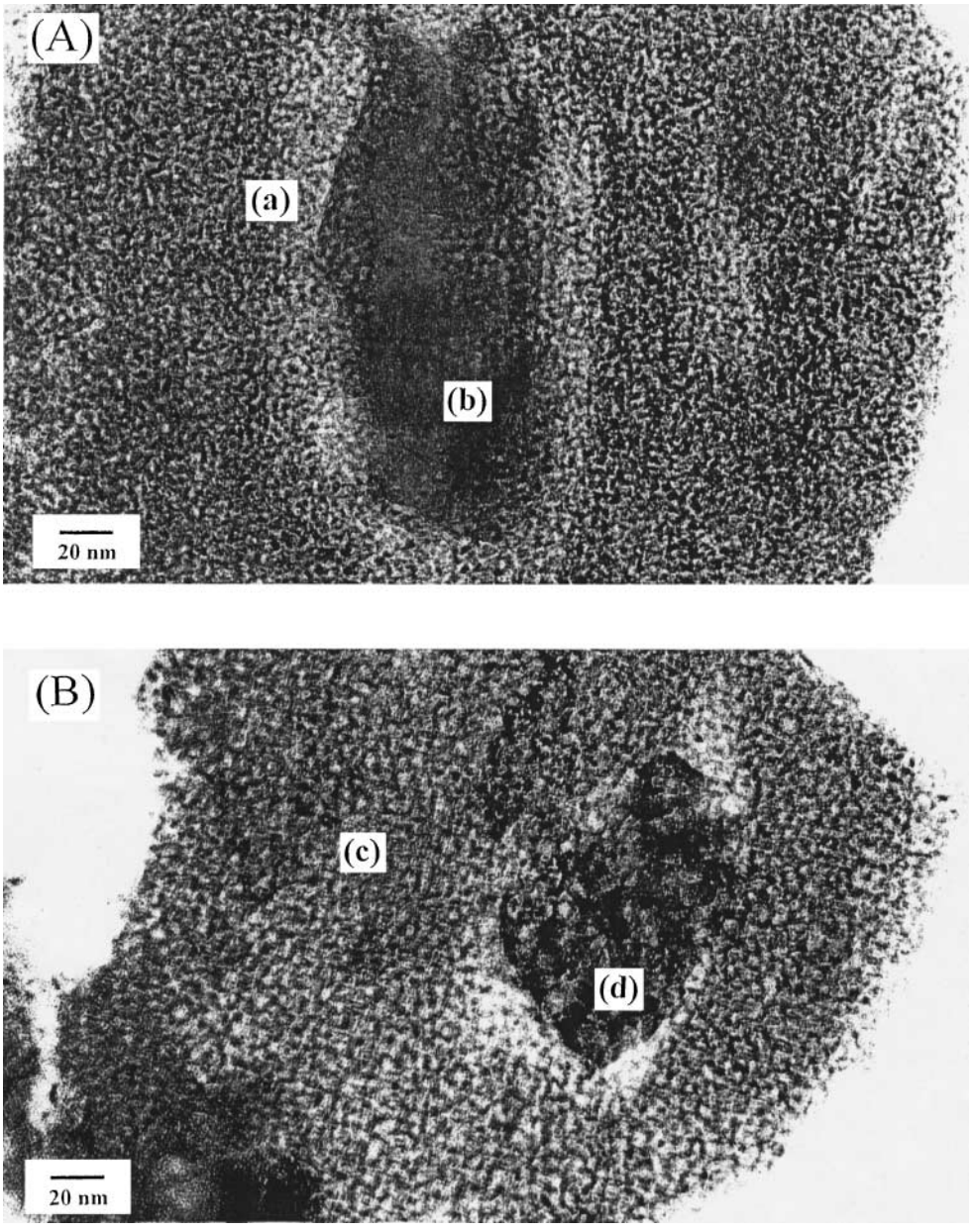

FIG. 3. TEM micrographs of (A) 25A923, (B) 25A1023, and (C) 50A973.

the parent oxide precursors on the formation of the cobalt molybdenum nitride. The 25AF723, 25BF723, and 25CF723 catalysts (Figs. 2A–2C) contained MoO_3 and $CoMoO_4$, while 25DF723 (Fig. 2D) consisted of MoO_3 and CoO in the precursor mixture. This shows that $CoMoO_4$ was formed during the oxidation of either cobalt nitrate or ammonium heptamolybdate as the starting material at 723 K. Co_3Mo_3N (Figs. 2F and 2G) was clearly formed in 25B973 and 25C973 and a small amount in 25A973 (Fig. 2E) by the nitridation of cobalt nitrate and/or ammonium heptamolybdate, but γ-Mo_2N and cobalt metal without Co_3Mo_3N were formed in 25D973 (Fig. 2H) by nitriding CoO and MoO_3. Thus, Co_3Mo_3N was not obtained by the nitridation of the mixture of CoO and MoO_3 but by the nitridation of $CoMoO_4$.

Morphology of Cobalt Molybdenum Nitrides

The morphologies of the 25A923, 25A1023, and 50A973 catalysts were determined by TEM and EDS measurements and are shown in Figs. 3 and 4, respectively. Figure 3A shows that sample 25A923 is composed of large particles (b) surrounded by a large number of small particles ((a), ca. 4 nm). This particle size was close to the crystallite size, Dc, of 4.5 nm obtained from XRD (Table 2). The EDS analysis (Fig. 4A) showed that particles (a) and (b) exhibited

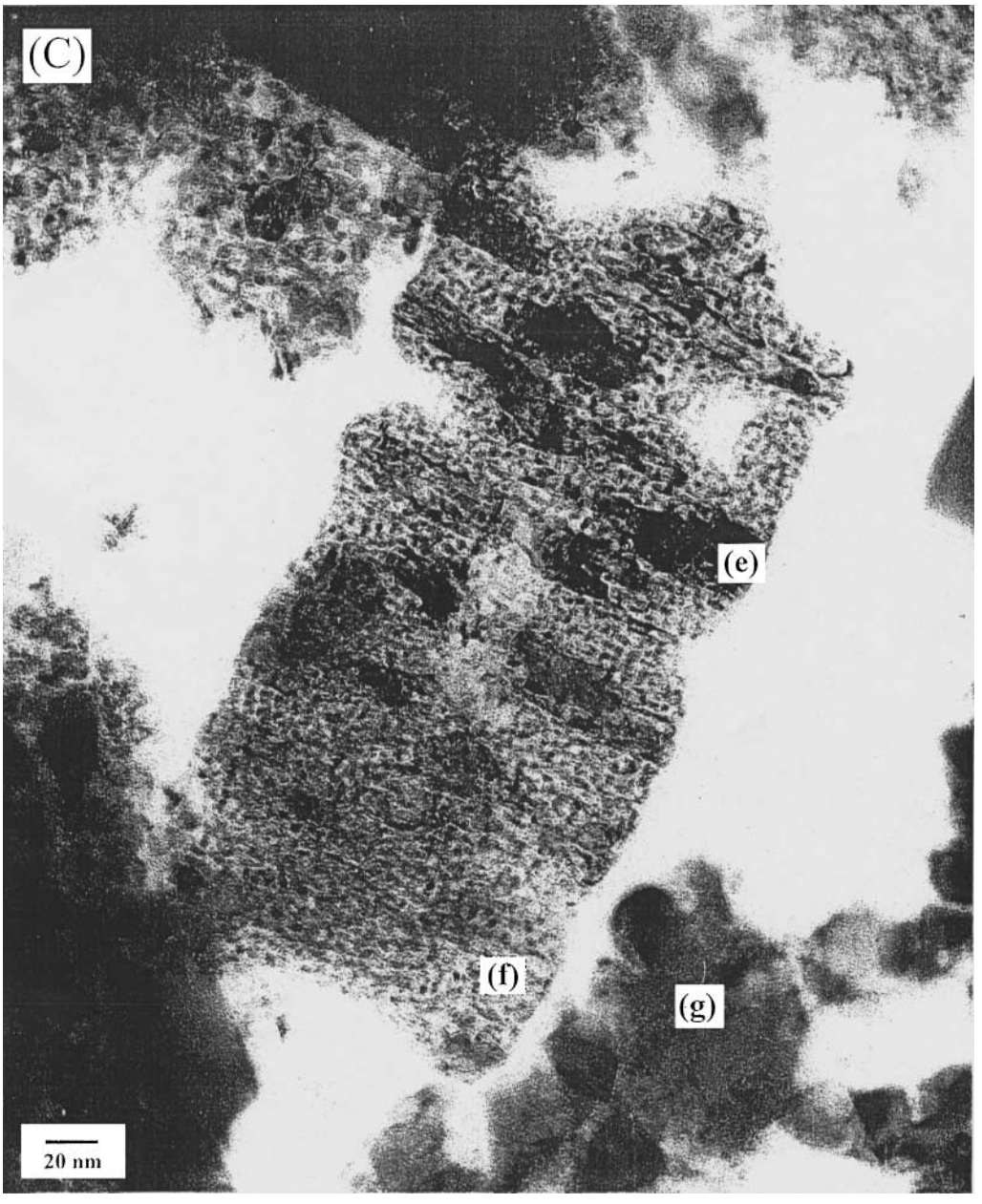

FIG. 3—*Continued*

Co/Mo ratios of (a) 0.01 and (b) 0.07, respectively, thus proving that these particles mainly contained γ-Mo_2N. Furthermore, Fig. 3B shows that 25A1023 contained large particles (d) of 20 to 30 nm (Dc of 15.9 nm by XRD) surrounded by a number of small particles (c). The Co/Mo ratio of the particles (d) was 0.22, which is a long way from unity, although the XRD patterns indicate the formation of Co_3Mo_3N in 25A1023. Therefore, the low Co/Mo ratio (0.22) is probably due to the presence of one slab of Co_3Mo_3N together with three slabs of γ-Mo_2N particles. Thus, the particles (d) contained Co_3Mo_3N, which appeared to be relatively large, flat crystallites. In Fig. 3C, the particles (e) of the 50A973 catalyst exhibit the highest Co/Mo ratio (3.5) and consist of Co nitride with Co_3Mo_3N as revealed by the TEM image. The particles (f) (C/Mo = 0.35, ca. 4 nm) had a particle size similar to that of γ-Mo_2N. Therefore, the particles contained γ-Mo_2N with Co nitride. Furthermore, based on the TEM image, the size of the particles (g) was about 20 nm, which was similar to a D_C of 30.3 nm after the XRD analysis. The Co/Mo ratio of (g) was 0.9, suggesting that the particles were composed of Co_3Mo_3N. Highly crystalline Co_3Mo_3N species were observed in 50A973. In the 25A923 and 25A1023 samples, small molybdenum nitride particles were formed and surrounded the crystallite

TABLE 3

The Surface Properties and Data for Thiophene HDS on Various Cobalt Molybdenum Nitrides and Sulfides

Catalyst	Irreversible CO uptake (μmolg^{-1})	Site density (atom nm^{-2})	S_{BET} ($m^2\,g^{-1}$)		HDS rate[b] (μmol min^{-1} g^{-1})		TOF[c] (min^{-1})	*n*-butane distribution (%)
			Before[a]	After[a]	0.167 h	8 h		
25A773	166	3.8	59	21	119	80.2	0.32	64
25A873	265	1.6	101	91	97.8	58.7	0.37	60
25A923	243	1.0	150	75	63.7	32.5	0.26	53
25A973	166	0.8	124	45	86.6	53.4	0.52	54
25A1023	101	1.3	47	50	48.4	36.1	0.48	50
25A1073	35	0.5	40	21	29.8	14.8	0.85	46
25S623	25	5.1	3	1	47.3	28.1	1.9	39
25AS623	38	0.4	66	40	68.0	32.0	1.8	40
25B973	786	8.2	58	—	71.0	33.8	0.09	52
25C973	277	1.6	107	—	50.3	24.3	0.18	47
0A973[d]	372	2.1	112	74	67.3	50.5	0.19	60

[a] Before and after the HDS reaction.
[b] At 623 K and atmospheric pressure.
[c] Mol converted thiophene/mol CO s^{-1}.
[d] Reference 4.

of γ-Mo_2N and Co_3Mo_3N. The presence of cobalt at small amount probably prevented crystal growth of γ-Mo_2N and Co_3Mo_3N.

BET Surface Area and Pore Distribution

Figure 5 shows the BET surface areas for A773-1073 with ratios of Co/(Co + Mo) = 0, 0.25, and 0.5. Table 3 lists the surface areas of the nitrided catalysts. The surface area of the samples increased from 59 $m^2\,g^{-1}$ for 25A773 to 150 $m^2\,g^{-1}$ for 25A923 and then decreased to 40 $m^2\,g^{-1}$ for 25A1073. The surface area of the catalysts (25A773-1073) showed a volcano-type curve with nitriding temperature and a maximum value (150 $m^2\,g^{-1}$) for 25A923. As expected, the 25A923 catalyst with the highest surface area had very small particles (4 nm), while the 25A1023 and 25A1073 catalysts had large particles (less than 20 nm) with small surface areas. The surface area of 25A975 (124 $m^2\,g^{-1}$) was relatively not as low as that of 25A923. The 25A1023 and 25A1027 catalysts containing Co_3Mo_3N had a larger surface area than those reported previously of 11 (12) and 66 (3). However, the surface areas of the samples without Co_3Mo_3N were larger than those of the catalysts: 103 $m^2\,g^{-1}$ for the Co–Mo oxynitride nitrided at 892 K (5), 148 for the catalyst nitrided at 883 K (10), 150 for 25A923, and 194 for the 4.8% Co 95.2% Mo catalyst nitrided at 973 K (8). In Fig. 6, the distributions of the micropores (Fig. 6A) and mesopores (Fig. 6B) for (a) 0A923, (b) 25A923, and (c) 25A1023 are shown. The 25A923 catalyst (b) exhibited a larger micropore volume than 0A923, indicating that the presence of cobalt increased the pore structure. The micropores and mesopores of the catalyst nitrided at 923 K were larger than those of the catalyst nitrided at 1023 K. Thus, the nitriding treatment at 1023 K made the crystallines of Co_3Mo_3N and β-$Mo_2N_{0.78}$ grow and thereby shrink the pore structure of the molybdenum nitride.

Determination of Cobalt Molybdenum Nitride and Water by TPR

The formation of Co_3Mo_3N on the surface of the catalysts nitrided at 973 to 1073 K during the TPR measurement is shown in Fig. 7. Ammonia and nitrogen were desorbed during the TPR. For the desorption of ammonia, the peak shape for 25A1023 (Fig. 7C) was analogous to that of 50A973 (Fig. 7D) (which contains Co_3Mo_3N) with a broad peak above 900 K. However, the 25A973 catalyst (Fig. 7B) had two peaks at about 600 and 800 K, which were different from those for 25A1023 and 50A973. Since the desorption peaks of ammonia at about 600 and 800 K were due to the adsorbed NH_X on the surface of γ-Mo_2N (17–20), the 25A973 catalyst was comprised of γ-Mo_2N on the surface. For 25A1023 and 50A973, the ammonia desorption was probably due to the NH_X species adsorbed on Co_3Mo_3N (Figs. 7C and D). Moreover, the nitrogen desorption profile for 0A973 (Fig. 7A) (γ-Mo_2N from XRD) exhibited three peaks at about 900, 1100, and 1200 K (17–20); the release from adsorbed NH_X, the transformations from γ-Mo_2N to β-$Mo_2N_{0.78}$ and from β-$Mo_2N_{0.78}$ to Mo metal. The 25A973 (Fig. 7B) catalyst did not show the significantly characteristic three peaks, but peaks smaller than 0A973. The nitrogen desorption profile for 25A973 above 1200 K was similar to that for 25A1023 (Fig. 7C). As a result, the 25A973 catalyst probably contained a small amount of Co_3Mo_3N and γ-Mo_2N. Furthermore, for the 100A973 catalyst (Fig. 7E) the broad nitrogen desorption peaks above 1100 K

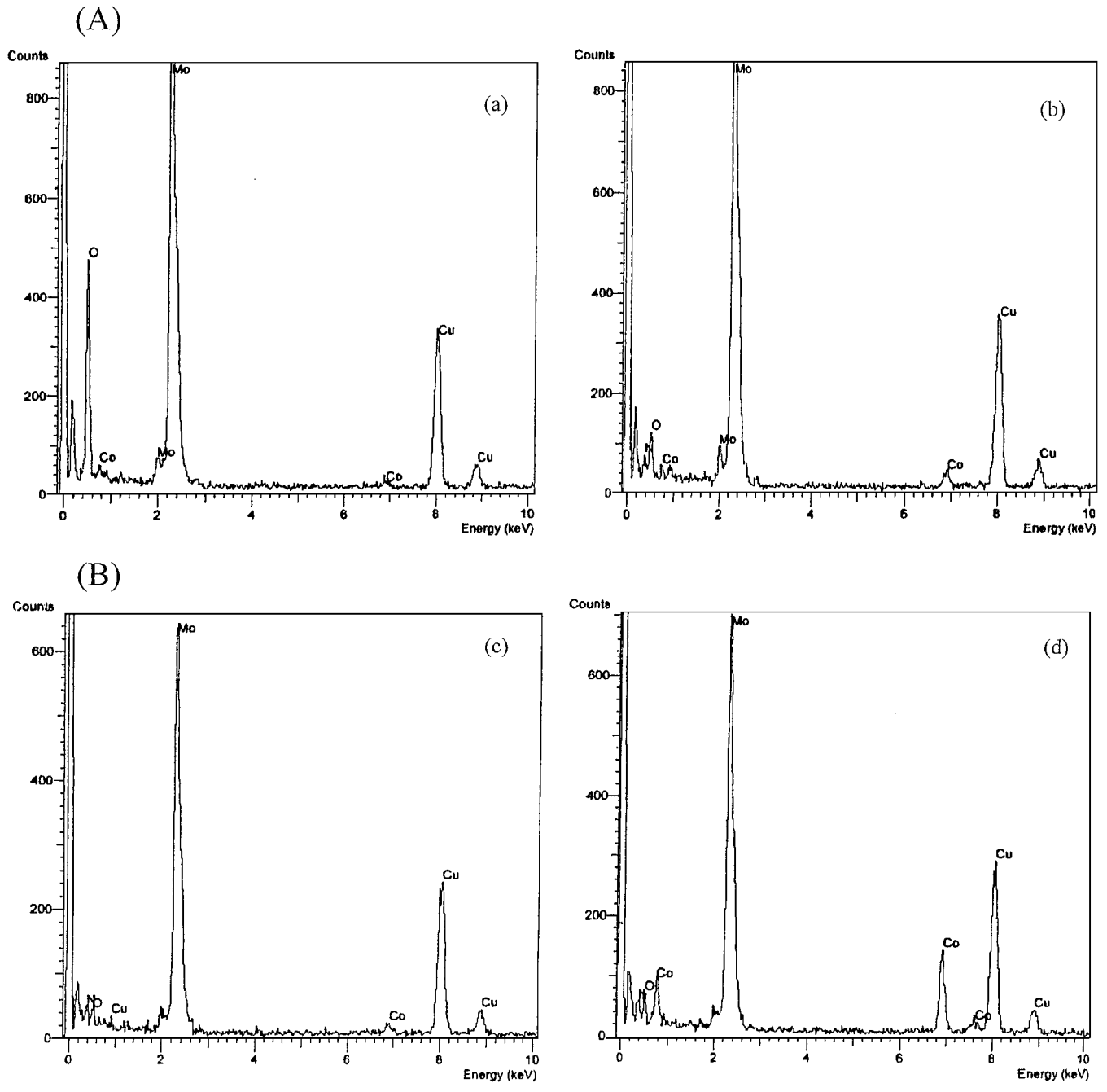

FIG. 4. EDS spectra of (A) 25A923, (B) 25A1023, and (C) 50A973. The letters (a)–(g) correspond to the particles indicated in Figs. 3A–3C.

and the peaks of ammonia desorption at about 700 and 1050 K were different from the peaks in Figs. 7A–7D. This suggests that Co nitride was formed on the surface of the 100A973 catalyst, as reported by Milad *et al.* (26). Therefore, γ-Mo_2N with a small amount of Co_3Mo_3N was mainly present on the surface of 25A973, Co_3Mo_3N on the surfaces of 25A1023 and 50A973, and cobalt nitride on the surface of 100A973. Furthermore, water was slightly formed in the catalysts (Figs. 7B–7E) compared to 0A973 during TPR, suggesting that the cobalt containing catalysts nitrided at 973 K was likely to contain a small amount of Co–Mo oxynitride and cobalt oxide.

Oxidation States of Cobalt Molybdenum Nitride

The distribution of the oxidation states of molybdenum and cobalt of the 25A773-1023 catalyst as obtained from the XPS measurements as a function of nitriding temperature

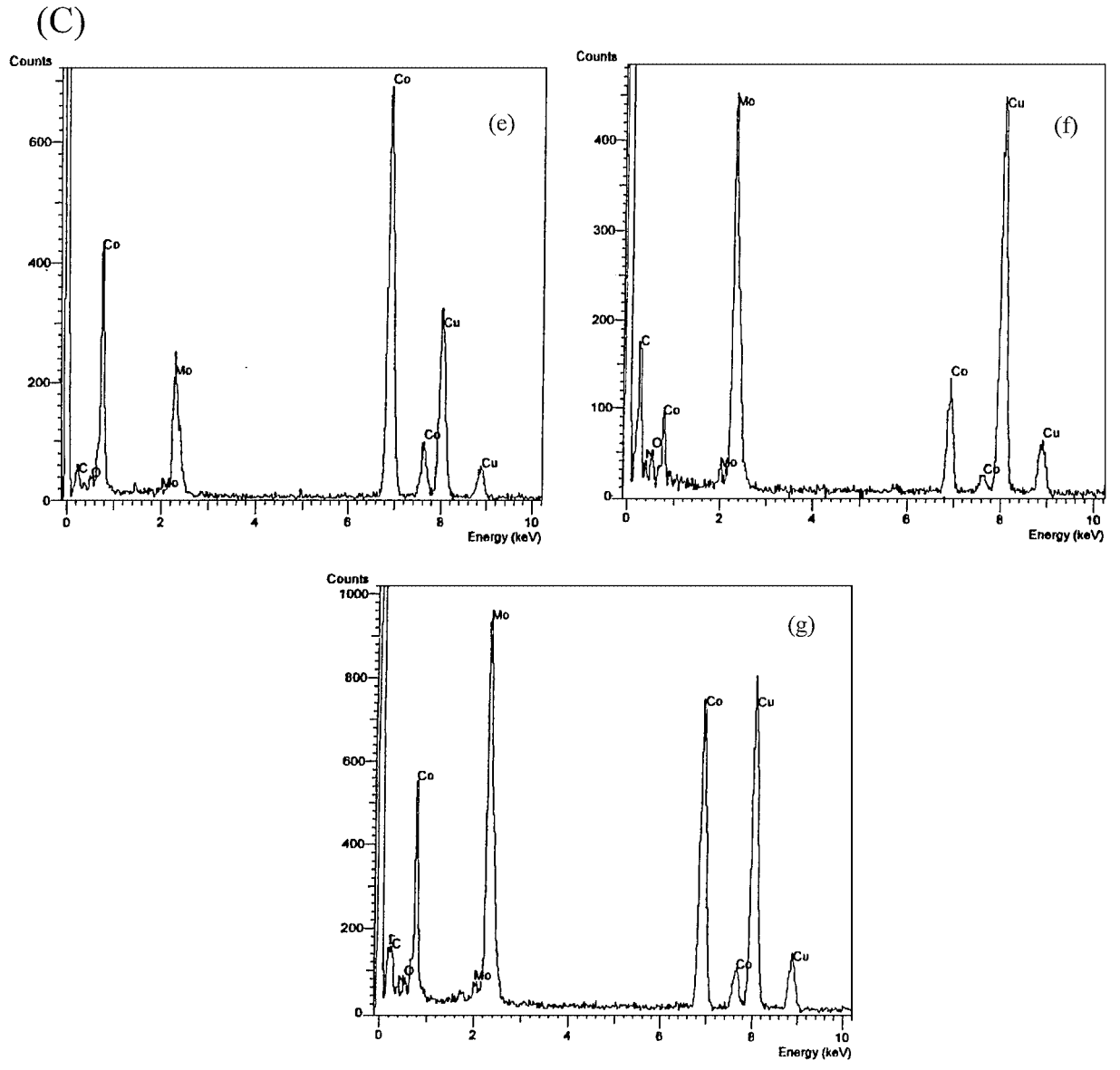

FIG. 4—*Continued*

is shown in Figs. 8A and 8B, respectively. Mo^{2+} and Mo^{0} were predominant in the Mo species and Mo^{0} increased above 923 K. The Mo^{3+}, Mo^{4+}, and Mo^{5+} contents were below 12%, regardless of the nitriding temperature. For the Co species, Co^{2+} was predominant with low percentages of Co^{0} and Co^{3+}, which gradually increased with increasing nitriding temperature. Co^{2+} was mainly present at all nitriding temperatures, even nitriding at 1023 K. This is probably due to the formation of cobalt oxide and Co–Mo oxynitride as well as the coexistence of various Co and Mo species on the surface. From the XRD analysis, the formation of γ-Mo_2N ($2\theta = 37.4$ and 43.5°), β-$Mo_2N_{0.78}$ (37.8 and 42.9°), Co_3Mo_3N (35.5 and 42.6°), and MoO_2 (36.9°) probably concealed the presence of CoO (36.7 and 42.3°) and Co–Mo oxynitride (37 and 43°). The catalysts were not exposed to air in the procedure from catalyst nitriding to placement into the XPS prechamber. Cobalt oxide could not be completely nitrided but remained in the oxide state under the conditions of this nitriding treatment. Furthermore, since molybdenum nitrides contained $Mo^{\delta+}$ ($\delta = 0$ and 2 (20, 24) and $0 < \delta < 4$ (7, 22, 23)), the Mo atomic valence of Co_3Mo_3N also exhibited $Mo^{\delta+}$ ($\delta \leq 2$). Therefore, the 25A773 and 25A873 catalysts, which contain MoO_2 and γ-Mo_2N according to XRD, mainly contained Mo^{2+}, Mo^{3+}, and Co^{2+}, while the 25A973 sample contained Mo^{0}, Mo^{2+}, Co^{0}, and Co^{2+} (Co_3Mo_3N and γ-Mo_2N by XRD). Co^{0} was mainly formed with Mo^{0} at 1023 K, suggesting the formation of Co nitride and Co_3Mo_3N in the catalyst.

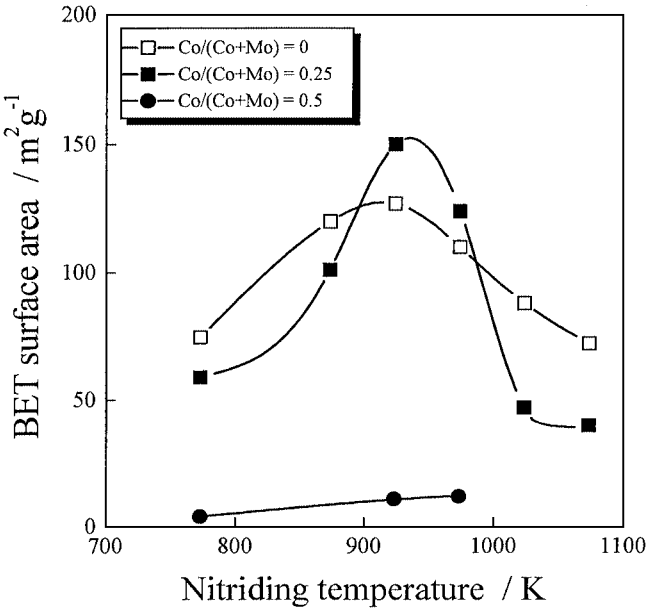

FIG. 5. Relationship between BET surface area and nitriding temperature.

Activity of Cobalt Molybdenum Nitrides for Thiophene HDS

Figure 9 shows the rates of the HDS of thiophene over various catalysts with Co/(Co + Mo) = 0.25 at 623 K as a function of time on stream. The 25A773 catalyst was the most active, while the 25A1073 catalyst was the least active. The 25A773-973 catalysts exhibited HDS rates higher than the 25S623 catalyst from sulfiding 25AF723 ($CoMoO_4$ by XRD). The HDS rates for 25A873-923 and 25S623 gradually decreased and reached a steady state after 4 h on stream, but the rate for 25A973 gradually increased after 3 h on stream. The 25A973 was more active than the 25A923. The higher activity of 25A973 than 25A923 is probably due to the presence of a small amount of

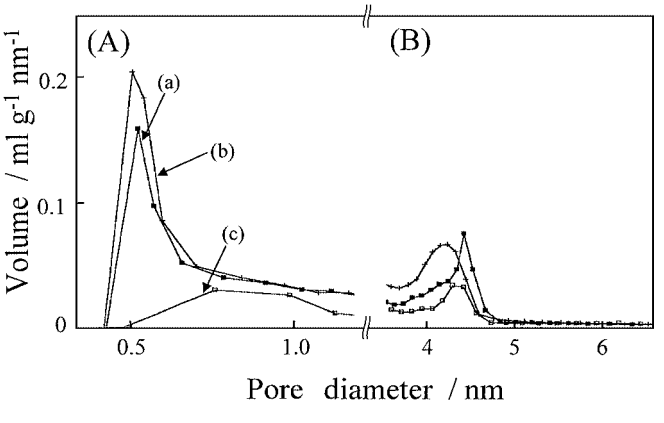

FIG. 6. Pore size distribution of (A) micropore region and (B) mesopore region for the (a) 0A923, (b) 25A923, and (c) 25A1023 catalysts.

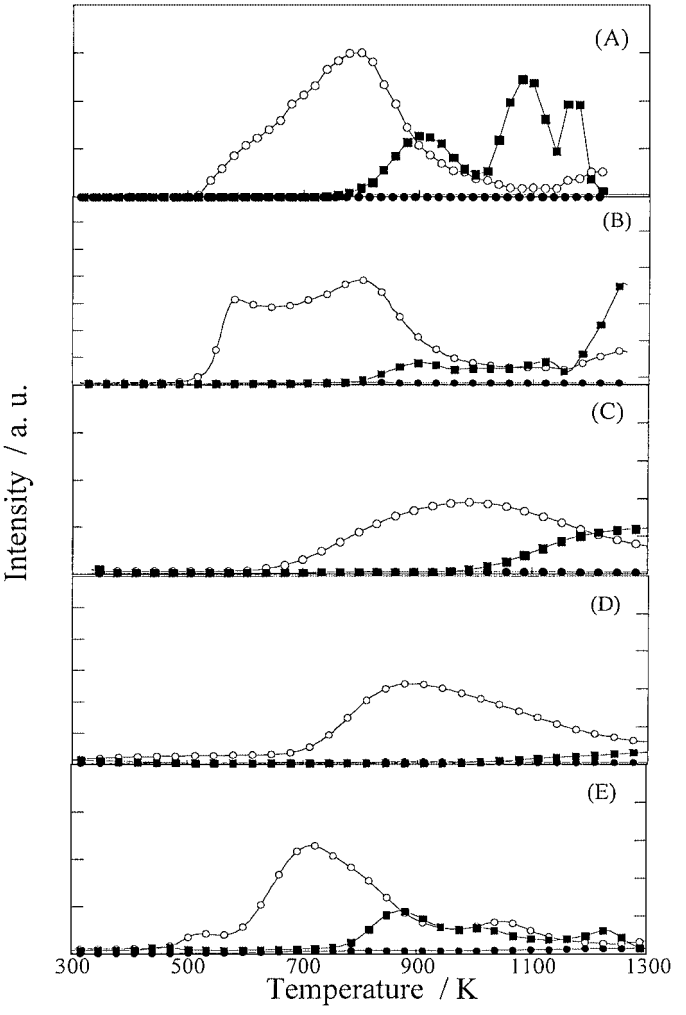

FIG. 7. TPR spectra of (A) 0A973, (B) 25A973, (C) 25A1023, (D) 50A973, and (E) 100A973. Symbols are (○) NH_3, (■) N_2, and (●) H_2O.

Co_3Mo_3N before the reaction and its obvious formation after the HDS reaction (Fig. 10). The reaction products were *n*-butane, 1-butene, *cis*-2-butene, and *trans*-2-butene. *n*-Butane made up 64% of the reaction products for 25A773, 54% for 25A973, and 39% for the 25S623. The product distribution of the butenes for thiophene HDS over the catalysts was close to that predicted for the thermodynamic equilibrium: *cis*-2-butene/*trans*-2-butene = 0.73–0.77 and 1-butene/2-butene = 0.33.

The cobalt molybdenum nitrides with Co/(Co + Mo) = 0.25, prepared by different methods, were tested for thiophene HDS as shown in Table 3: 25A973 (from $Co(NO_3)_2 \cdot H_2O$ and $(NH_4)_6Mo_7O_{24} \cdot 4H_2O$), 25B973 (from $Co(NO_3)_2H_2O$ and MoO_3), and 25C973 (from CoO and $(NH_4)_6Mo_7O_{24} \cdot 4H_2O$). The 25A973 catalyst was about 1.6 and 2.2 times more active than the other two catalysts after 8 h on stream, indicating that the mixture of cobalt nitrate and ammonium molybdate was a good precursor

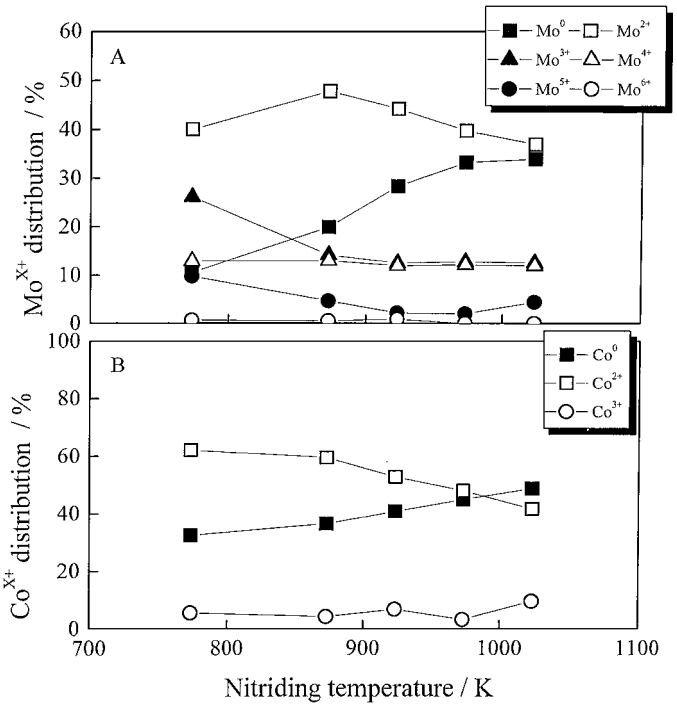

FIG. 8. The relationship between the distribution of (A) Mo^{x+} ions and (B) Co^{x+} ions in the samples and nitriding temperature.

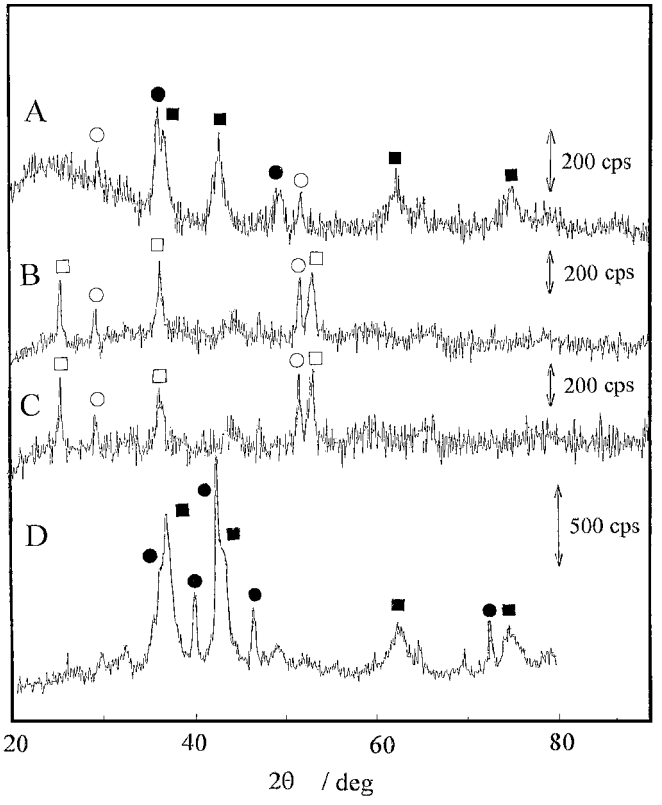

FIG. 10. XRD patterns of (A) 25AS623 and (B) 25S623 before the reaction, (C) 25S623 after the reaction, and (D) 25A973 after the reaction. Symbols are (●) Co_3Mo_3N, (■) γ-Mo_2N, (□) MoO_2, and (○) Co_9S_8.

for an active HDS CoMo nitride catalyst compared to the precursors prepared with CoO and/or MoO_3. The HDS rate of 25A973 was 1.3 (at 0.167 h) times more active than the unsupported γ-Mo_2N (0A973) and was reported to be the most active of the CoMo catalysts with various cobalt loadings (4). Thus, the HDS activity (per catalyst weight) depended on the composition (Co/(Co + Mo)) of the cobalt molybdenum nitrides. Kim *et al.* (3) also found a higher activity for the cobalt molybdenum nitride with Co/(Co + Mo) = 0.25 during thiophene HDS compared to the other compositions. Ihm *et al.* (9) reported that unsupported CoMo nitride with Co/(Co + Mo) = 0.5 was less active than Mo nitride.

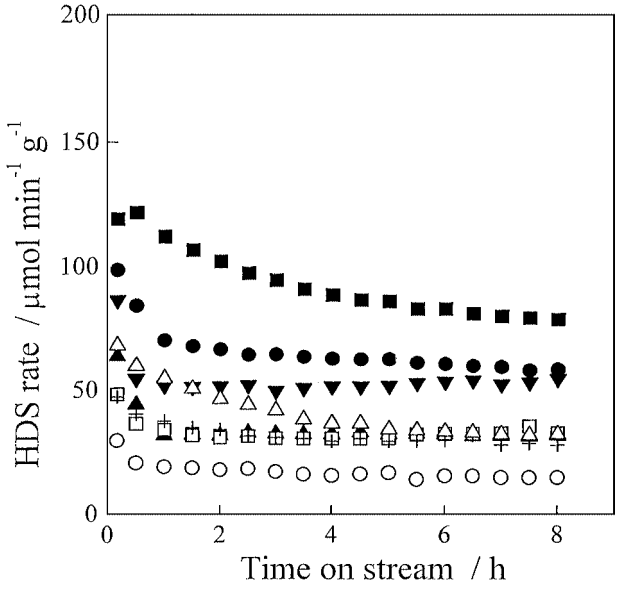

FIG. 9. The rate of thiophene HDS over the cobalt–molybdenum nitride catalysts with Co/(Co + Mo) = 0.25 as a function of nitriding temperature and 25S625 catalyst: (■) 25A773, (●) 25A873, (▲) 25A923, (▼) 25A973, (□) 25A1023, (○) 25A1073, (+) 25S623, and (△) 25AS623.

A comparison of the CoMo nitrides with the CoMo sulfides showed that the HDS rates for the 25S623 and 25AS623 catalysts were 53 and 60%, respectively, lower than that of 25A973. Ihm *et al.* (9) also reported that the sulfidation of the unsupported Co_3Mo_3N at 673 K significantly decreased by 22% the activity of Co_3Mo_3N. As shown in Table 3, the HDS rate for 25A973 changed from 87 to 53 μmol min^{-1} g^{-1} with a surface area change of 124 to 45 m^2 g^{-1} during the reaction. Furthermore, the surface areas of the 25S623 and 25AS623 catalysts significantly decreased from 3 to 1 m^2 g^{-1} and from 66 to 40 m^2 g^{-1}, respectively. On a surface area basis, the HDS rate of the 25S623 catalyst was significantly higher than that of the other nitrided catalysts. Thus, the HDS activities of the unsupported cobalt molybdenum nitride catalysts (per catalyst weight), with and without sulfidation, were significantly affected by

the surface area as well as by the composition of the nitride catalysts. In contrast, Logan *et al*. (11) prepared sulfided and reduced $CoMoO_4/Al_2O_3$ and Co_3Mo_3N/Al_2O_3 catalysts ($Co/(Co+Mo)=0.25$), which were passivated in 1% O_2/He and subsequently reduced in a stream of hydrogen at 750 K. They reported that the sulfidation of the $CoMoO_4/Al_2O_3$ and Co_3Mo_3N/Al_2O_3 catalysts at 623 K remarkably improved the thiophene HDS activity measured at 693 K after 24 h. The activity of the unsupported sulfided CoMo nitride catalyst (25AS623) was higher than the activity of the 25A973 catalyst during the initial stage of the reaction and approached the same activity as the 25S623 after 8 h. Moreover, the HDS rate for 25A973 gradually increased after 3 h of the reaction. The higher activity of the 25AS623 during the initial stage and that of 25A973 after 3 h was probably related to the improved activity of the supported CoMo nitride in Logan's study. The XRD patterns before and after reaction are shown in Fig. 10. Co_3Mo_3N was prominently formed in 25A973 after the reaction, although Co_3Mo_3N was slightly observed before the reaction. The γ-Mo_2N phase of 25A973 remained upon the formation growth of Co_3Mo_3N crystals under the HDS conditions but no Co_9S_8 was formed. 25S623 contained MoO_2 ($2\theta=36.9^\circ$) and Co_9S_8 before the reaction. However, 25AS623 did not contain MoO_2 but Co_9S_8 before the reaction. As a result, the sulfidation decreased the activity to a greater extent than that 25A973 due to the Co_9S_8 formation. 25S623 was to an extent less active than 25A973 and 25AS623 due to the formation of MoO_2. Thus, the formation of MoO_2 and Co_9S_8 led to a decrease in the HDS activity of the catalysts.

The CO chemisorption capacities of the CoMo nitride and sulfide catalysts were used to normalize the activities of the cobalt molybdenum species for the thiophene HDS ($TOF_{integral}$); these results are shown in Table 3. Although the CoMo nitride and sulfide catalysts contained a variety of Co and Mo species, as indicated by the XRD and XPS results, the $TOF_{integral}$ probably provides a better understanding of the surface active species for thiophene HDS over the CoMo catalysts than the activities per catalyst weight. The CO adsorption of the CoMo catalysts decreased with increasing nitriding temperature. This is in agreement with the results obtained from the irreversible CO measurements for the passivated/reduced 12.5 wt% Mo/Al_2O_3 nitrided at 973 K (cooled in NH_3 after nitriding) (20) and 97.3 wt% MoO_3/Al_2O_3 (purged and cooled in He after nitriding) (19) catalysts. The 25A773 and 25A873 catalysts exhibited high HDS rates and high site densities for the CO adsorption, but the $TOFs_{integral}$ were only 40% lower than those of the 25A1073 catalyst. Therefore, the 25A773 and 25A873 catalysts contained a number of weak active sites ($TOF_{integral}$ 0.32 and 0.37 min^{-1}). The 25A773 catalyst consisted of MoO_2 (and CoO) (mainly Mo^{2+} and Co^{2+} with Mo^{3+} and Mo^{4+}), while the 25A873 catalyst contained γ-Mo_2N and MoO_2 (and CoO) (mainly Mo^{2+}, Mo^0, and Co^{2+} with Mo^{3+} and Mo^{4+}). The 25A923 catalyst did not exhibit a very high rate of HDS, even though it had a high surface area and showed a high CO uptake. As a consequence, it had a low $TOF_{integral}$. This catalyst contained γ-Mo_2N (Co-Mo oxynitride) with MoO_2, which formed less active sites on the surface. The 25A973 catalyst had a 2.7- and 2.0-fold higher $TOF_{integral}$ than 0A973 (γ-Mo_2N) and 25A923, respectively, showing that Co_3Mo_3N was more active than γ-Mo_2N. In contrast, the 25A1023 and 25A1073 catalysts had low HDS rates but high $TOF_{integral}$ values. These catalysts contained Co_3Mo_3N and a small number of highly active sites. The 25B973 catalyst also had larger (10- and 15-fold) site densities than the 25A973 and 25C973 catalysts, and a $TOF_{integral}$ substantially lower than those of 25A973 and 25C973. This result suggested that the 25B973 catalyst had a number of weak active sites (γ-Mo_2N) because Co_3Mo_3N with a high $TOF_{integral}$ was formed in a small amount. Thus, the oxidic precursors influenced the formation of the active sites on the cobalt molybdenum nitride catalysts. Furthermore, the $TOFs_{integral}$ of the 25S623 and 25AS623 catalyst were 3.7 and 3.4 times higher than that of 25A973, respectively, during thiophene HDS after 0.167 h on stream. Consequently, the sulfidation probably produces stronger active sites on the CoMo sulfide (or sulfnitride (11)) compared to Co_3Mo_3N for the HDS reaction. The CoMo sulfide and sulfided Co_3Mo_3N exhibited the highest $TOF_{integral}$, followed by Co_3Mo_3N based on CO adsorption. Furthermore, for the alumina-supported CoMo nitride/sulfide catalyst, the high density of more active sites may increase in a layer of highly dispersed CoMo sulfnitride on the surface of alumina under the reaction conditions compared to the bulk CoMo catalysts (11).

CONCLUSIONS

γ-Mo_2N (oxynitride) formed together with a small amount of Co_3Mo_3N at 973 K, while γ-Mo_2N (oxynitride) formed with MoO_2 at 873 K. Co_3Mo_3N formed together with γ-Mo_2N during nitridation at 1023 K. Co_3Mo_3N, γ-Mo_2N, β-$Mo_2N_{0.78}$, Mo metal, and Co nitride, formed during the nitriding at 1073 K. The rate of thiophene HDS per catalyst weight depended on the composition (Co/Mo) and surface area. The 25A973 had a higher HDS rate and $TOF_{integral}$ than 25A923, showing that Co_3Mo_3N was more active than γ-Mo_2N. The 25A1023 and 25A1073 catalysts had low HDS rates but high $TOF_{integral}$ values. The 25A873 catalyst exhibited only a 40% lower activity than that of the 25A1073 catalyst, thus 25A873 contained a number of weak active sites. In these catalysts, Co_3Mo_3N formed with a small number of highly active sites in the catalysts. The sulfidation of 25A973 and 25AF723 produced stronger active sites for the CoMo sulfide (or sulfnitride) rather than Co_3Mo_3N.

ACKNOWLEDGMENTS

We are grateful to T. Watabe and Y. Kondo (JEOL HIGH TECH, JEOL, Co., Ltd., Tokyo, Japan) for TEM analyses.

REFERENCES

1. Bem, D. S., Gibson, C. P., and zur Loye, H.-C., *Chem. Mater*. **5**, 397 (1993).
2. Jackson, S. K., Layland, R. C., and zur Loye, H.-C., *J. Alloys Compd*. **291**, 94 (1999).
3. Kim, D.-W., Lee, D.-K., and Ihm, S.-K., *Catal. Lett.* **43**, 91 (1997).
4. Hada, K., Nagai, M., and Omi, S., *J. Phys. Chem. B* **105**, 4084 (2001).
5. Yu, C. C., Ramanathan, S., and Oyama, S. T., *J. Catal.* **173**, 1 (1998).
6. Ramanathan, S., Yu, C. C., and Oyama, S. T., *J. Catal.* **173**, 10 (1998).
7. Park, H. K., Lee, J. K., Yoo, J. K., Ko, E. S., Kim, D. S., and Kim, K. L., *Appl. Catal. A* **150**, 21 (1997).
8. Kojima, R., and Aika, K., *Chem. Lett.* 514 (2000).
9. Ihm, S.-K., Kim, D.-W., and Lee, D.-K., *Stud. Surf. Sci. Catal.* **111**, 343 (1997).
10. Li, Y., Zhang, Y., Raval, R., Li, C., Zhai, R., and Xin, Q., *Catal. Lett.* **48**, 239 (1997).
11. Logan, J. W., Heiser, J. L., McCrea, K. R., Gates, B. D., and Bussell, M. E., *Catal. Lett.* **56**, 165 (1998).
12. Jacobsen, C. J. H., *Chem. Commun.* 1057 (2000).
13. Miga, K., Stanczyk, Sayag, C., K., Sayag, C., Brodzki, D., and Djéga-Mariadassou, G., *J. Catal.* **183**, 63 (1999).
14. Claridge, J. B., York, A. P. E., Brungs, A. J., and Green, M. L. H., *Chem. Mater.* **12**, 132 (2000).
15. Chu, Y., Wei, Z., Yang, S., Li, C., Xin, Q., and Min, E., *Appl. Catal. A* **176**, 17 (1999).
16. Herle, P. S., Hegde, M. S., Sooryanarayana, K., Row, T. N. G., and Subbanna, G. N., *Inorg. Chem.* **37**, 4128 (1998).
17. Nagai, M., Miyata, A., Kusagaya, T., and Omi, S., *in* "The Chemistry of Transition Metal Carbides and Nitrides" (S. T. Oyama, Ed.), p. 327. Blackie, London, 1996.
18. Hada, K., Nagai, M., and Omi, S., *J. Phys. Chem B* **104**, 2090 (2000).
19. Nagai, M., Goto, Y., Miyata, A., Kiyoshi, M., Hada, K., Oshikawa, K., and Omi, S., *J. Catal.* **182**, 292 (1999).
20. Nagai, M., Goto, Y., Irisawa, A., and Omi, S., *J. Catal.* **191**, 128 (2000).
21. Wei, Z., Xin, Q., Grange, P., and Delmon, B., *J. Catal.* **168**, 176 (1997).
22. Choi, J.-G., Brenner, J. R., Colling, C. W., Demczyk, B. G., Dunning, J. L., and Thompson, L. T., *Catal. Today* **15**, 201 (1992).
23. Ozkan, U. S., Zhang, L., and Clark, P. A., *J. Catal.* **172**, 294 (1997).
24. Nagai, M., Takada, J., and Omi, S., *J. Phys. Chem. B* **103**, 10180 (1999).
25. Juza, R., and Sachsze, W., Z. *Anorg. Chem.* **253**, 95 (1945).
26. Milad, I. K., Smith, K. J., Wong, P. C., and Mitchell, K. A. R., *Catal. Lett.* **52**, 113 (1998).
27. Oda, K., Yoshio, T., and Oda, Ko., *J. Mater. Sci.* **22**, 2729 (1987).
28. Quincy, R. B., Houalla, M., Proctor, A., and Hercules, D. M., *J. Phys. Chem.* **94**, 1520 (1990).
29. Pawelec, B., Navarro, R., Fierro, J. L. G., and Vasudevan, P. T., *Appl. Catal. A* **168**, 205 (1998).
30. Figueiredo, R. T., Granados, M. L., Fierro, J. L. G., Vigas, L., de la Piscina, P. R., and Homs, N., *Appl. Catal. A* **170**, 145 (1998).
31. Zsoldos, Z., Garin, F., Hilaire, L., and Guczi, L., *Catal. Lett.* **33**, 39 (1995).